HOKKAIDO UNIVERSITY

Title	Metabolism-Coupled Cell-Independent Acetylcholinesterase Activity Assay for Evaluation of the Effects of Chlorination on Diazinon Toxicity
Author(s)	Matsushita, Taku; Kikkawa, Yuji; Omori, Kei; Matsui, Yoshihiko; Shirasaki, Nobutaka
Citation	Chemical research in toxicology, 34(9), 2070-2078 https://doi.org/10.1021/acs.chemrestox.1c00155
Issue Date	2021-09-20
Doc URL	http://hdl.handle.net/2115/86540
Rights	This document is the unedited Author ' s version of a Submitted Work that was subsequently accepted for publication in Chemical research in toxicology, copyright c American Chemical Society after peer review. To access the final edited and published work see https://pubs.acs.org/articlesonrequest/AOR-RN9RYMPQ9PNBD4EY5JP6.
Type	article (author version)
File Information	for-HUSCAP_matsushita_2021.pdf

Instructions for use

Hokkaido University Collection of Scholarly and Academic Papers : HUSCAP

A metabolism-coupled cell-independent acetylcholinesterase activity assay for evaluation of the effects of chlorination on diazinon toxicity

Taku Matsushita[†*], Yuji Kikkawa[‡], Kei Omori[‡],
Yoshihiko Matsui[†], and Nobutaka Shirasaki[†]

[†]Faculty of Engineering, Hokkaido University, N13W8, Sapporo 060-8628, Japan

[‡]Graduate School of Engineering, Hokkaido University, N13W8, Sapporo 060-8628, Japan

[*]Corresponding author: taku-m@eng.hokudai.ac.jp; +81–11–706–7279

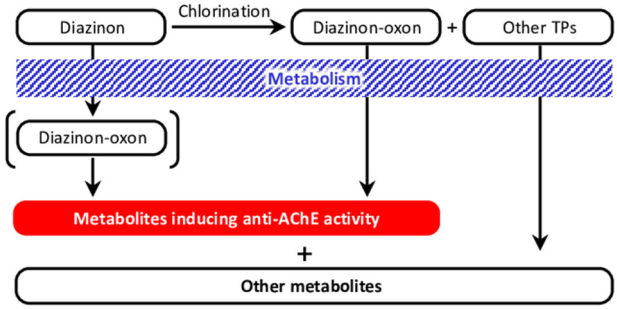

Abstract

Drinking water quality guideline values for toxic compounds are determined based on their acceptable daily intake. The toxicological endpoint for determining the acceptable daily intake of most organophosphorus insecticides is inhibition of acetylcholinesterase (AChE). Although insecticides ingested with drinking water are partly metabolized by the liver before transport to the rest of the body, no current cell-independent AChE activity assay takes the effects of metabolism into account. Here, we incorporated metabolism into a cell-independent AChE activity assay and then evaluated the change in anti-AChE activity during chlorination of a solution containing the organophosphorus insecticide diazinon. The anti-AChE activities of solutions of diazinon or diazinon-oxon, the major transformation product of diazinon during chlorination, were dramatically changed by metabolism: the activity of diazinon solution was markedly increased, whereas that of diazinon-oxon solution was slightly decreased, clearly indicating the importance of incorporating metabolism into assays examining toxicity after oral ingestion. Upon chlorination, diazinon was completely transformed, in part to diazinon-oxon. Although diazinon solution without metabolism did not show anti-AChE activity before chlorination, it did after chlorination. In contrast, with metabolism, diazinon solution did show anti-AChE activity before chlorination, but chlorination gradually decreased this activity over time. The observed anti-AChE activities were attributable solely to diazinon and diazinon-oxon having been contained in the samples before metabolism, clearly suggesting that the presence not only of diazinon, but also of diazinon-oxon, should be monitored in drinking water. Further examination using a combination of tandem mass spectrometry and *in silico* site-of-metabolism analyses revealed the structure of a single metabolite that was responsible for the observed anti-AChE activity after metabolism. However, because this compound is produced via metabolism in the human body after oral ingestion of diazinon, its presence in drinking water need not be monitored and

regulated.

Keywords: Drinking water; metabolite; oxon; transformation product.

1. Introduction

Organophosphorus insecticides are used in large quantities worldwide, despite their being banned in some countries due to concerns over their toxicity in humans. Organophosphorus insecticides contaminate river waters via agricultural runoff,[1-3] and as a result, drinking water treatment plants located downstream of farms are often forced to use contaminated river water for the production of drinking water. Because organophosphorus insecticides are not removed by conventional drinking water treatment processes (i.e., coagulation, sedimentation, and sand filtration),[4] they remain in the water when free chlorine is applied as the final treatment for disinfection. This leaves the organophosphorus insecticides to react with the free chlorine during distribution of finished water to businesses and households. Reaction with free chlorine transforms the organophosphorus insecticides mainly to their oxons via oxidation of a P=S bond to a P=O bond.[5-7] This transformation is reported to occur during other unit processes such as ozonation,[8, 9] UV irradiation,[10, 11] and advanced oxidation process.[12, 13] However, other transformation products, such as hydrolytes, are also reported to be produced during chlorination.[14, 15]

The presence of pesticides and their metabolites, including oxons, in drinking water,[16] and the production of pesticide transformation products by environmental or water treatment processes,[17-19] are issues that are attracting increasing attention worldwide due to their potential impacts on human health. When drinking water contaminated with an organophosphorus insecticide is ingested, the insecticide is absorbed by the small intestine and transported by the blood to the liver, where it is metabolized by drug-metabolizing enzymes. These metabolites, and any remaining unmetabolized insecticide, are then transported to the rest of the body. However, none of the currently available *in vitro* cell-independent AChE activity assays take this metabolism into account; that is, they evaluate only the direct impact of the target compound on AChE activity, which does not always reflect the actual toxicity in the human body after oral ingestion. Therefore, investigation of anti-AChE activity both with and without metabolism is required for evaluating the true toxicity of organophosphorus insecticides in humans.

Drinking water quality guideline values for organophosphorus insecticides are usually determined based on acceptable daily intake values, which are the amount of substance that can be safely ingested daily over a lifetime. The primary mode of action of organophosphorus insecticides is inhibition of the activity of acetylcholinesterase (AChE) at synapses; therefore, *in vivo* assays using AChE inhibition as the toxicological endpoint are most often used for determining acceptable daily intake values for organophosphorus insecticides. In the laboratory, however, *in vitro* assays are often preferred over *in vivo* assays for evaluating changes in the toxicity (i.e., changes in anti-AChE

activity) of organophosphorus insecticides during water treatment processes[20-23] because of their higher throughput and greater simplicity. However, unlike *in vivo* assays, these *in vitro* assays do not inherently take into account the effects of metabolism on toxicity. Many *in vitro* cell-independent assays for evaluating AChE activity have been developed. The most widely used is Ellman's assay, in which the yellow color caused by the reaction of thiocholine, which is produced by hydrolysis of acetylthiocholine by AChE, with a coloring reagent is measured as an index of AChE activity.[24] Several chemiluminescent probes have been developed as alternatives to the traditional coloring reagent, which have been shown to markedly increase the sensitivity of the assay.[25, 26] More recently, direct measurement of choline (Ch), which is produced from acetylcholine by AChE, by liquid chromatography–tandem mass spectrometry (LC–MS/MS) has been reported as a highly sensitive and high-throughput means of determining AChE activity.[27]

In vitro cell-independent AChE activity assays have been used in several studies to examine the changes in the anti-AChE activity of organophosphorus insecticides during chlorination; for example, for EPN (*O*-ethyl *O*-(4-nitrophenyl) phenylphosphonothioate),[23] malathion,[15] and methidathion,[15] their anti-AChE activities are reported to increase with chlorination time, even though the parent insecticides are completely transformed immediately upon chlorination. Further investigation of these increases by Matsushita et al.[15] revealed that the anti-AChE activity of solutions of malathion or methidathion after chlorination was attributable to their oxons alone, and that other transformation products that formed did not contribute to the observed anti-AChE activities. Because these oxons have the same mode of action (i.e., anti-AChE activity) but higher activity than their parent insecticides,[15, 28] Matsushita et al. suggested the need to include the oxons, but not the other transformation products, in drinking water guidelines. In the European Union and Japan, some oxons (as well as their parent insecticides) are already included in drinking water quality regulations. However, which oxons to include and whether or not other transformation products should be included in the regulations requires further investigation.

Accordingly, the objectives of the present study were (1) to develop an *in vitro* cell-independent AChE activity assay that takes into account the effects of metabolism, (2) to evaluate, using our assay, the changes in anti-AChE activity of diazinon, a widely-used representative organophosphorus insecticide, during chlorination with or without metabolism, and (3) to discuss the need to regulate the transformation products of diazinon produced by chlorination processes from the perspective of their contributions to the anti-AChE activity of solutions of diazinon. This is the first report in which the effects of metabolism were incorporated into the *in vitro* cell-independent AChE activity assay. Additionally, we found that metabolism markedly changed the anti-AChE activity of diazinon and diazinon-oxon, but that neither diazinon nor diazinon-oxon were responsible for the observed anti-AChE activity. Further examination using a combination of tandem mass spectrometry and *in silico* site-of-metabolism analyses revealed the structure of the single responsible metabolite.

2. Materials and Methods

2.1 Chemicals

Chemical standards of diazinon and diazinon-oxon (Fig. S1), S9, cofactors (glucose-6-phosphate, β-NADPH, and β-NADH), acetylcholine (ACh), and Ch were purchased from Fujifilm Wako Pure Chemical Corporation (Osaka, Japan). AChE derived from human erythrocytes was purchased from Merck KGaA (Darmstadt, Germany). Sodium hypochlorite (guaranteed reagent grade), which is used in full-scale water treatment plants, was purchased from AGC Inc. (Tokyo, Japan). All chemicals were used without any further purification.

2.2 Batch chlorination experiments

Diazinon was dissolved in 10 mM phosphate buffer (pH 7.0) to a concentration of 38 μM without the addition of organic solvents to avoid the solvents from affecting the experimental results as follows: a phosphate buffer was supplemented with diazinon chemical standard, stirred with a magnetic stirrer overnight, and then filtered through a PTFE membrane having pores of 0.45 μm in diameter to remove undissolved diazinon. The concentration of diazinon in the solution was then confirmed with LC–MS. Chlorination was conducted by adding sodium hypochlorite to the diazinon solution at a concentration of 12 mg-Cl_2/L, which was sufficient to maintain a free chlorine residual throughout the chlorination period, and then mixing with a magnetic stirrer for 10 min. After mixing, the glass vessel was tightly sealed with Parafilm and a screw-cap to avoid volatilization to the atmosphere and the mixture was left to rest at 20 °C in the dark for 168 h. During chlorination, aliquots of the mixture were withdrawn at predetermined intervals, residual chlorine in the samples was quenched with sodium sulfite, and the samples were subjected to AChE activity assay with or without metabolism, and to quantification of diazinon and diazinon-oxon by LC–MS.

2.3 Metabolism using S9 mix

The metabolic activation procedure with liver S9 used in the Ames assay[29] was applied prior to AChE activity assay. The S9 consists of microsomal and cytosolic fractions of a liver homogenate, possessing both phase I and phase II enzymatic activities.[30] A stock solution of S9 mix was prepared by dissolving the commercial S9 and cofactors (i.e., glucose-6-phosphate, β-NADPH, and β-NADH) in phosphate buffer (Table S1) on ice. Then, metabolism was induced by mixing 800 μL of test sample with 2000 μL of the S9 stock solution and incubating the mixture at 37 °C for 20 min in a shaking water bath. After metabolism, 900 μL of the sample was immediately centrifuged (19,200 × *g*) at 4 °C for 60 min in an ultracentrifuge (himac CP-60E, Eppendorf Himac Technologies Co., Ltd., Hitachinaka, Japan) to separate the S9 from diazinon and its derivatives. The resulting supernatant was subjected to AChE activity assay.

2.4 AChE activity assay

The *in vitro* LC-MS–based AChE activity assay reported previously[15] was used with slight modifications. In brief, an aliquot of 1 mM phosphate buffer (pH 7.4), prepared by dissolving Na_2HPO_4 and NaH_2PO_4 in Milli-Q water, was supplemented with NaCl at a concentration of 150 mM

(hereafter "assay buffer"). A working solution of AChE was prepared by adding AChE to the assay buffer at a concentration of 60 units/L, and a working solution of ACh was prepared by adding ACh to the assay buffer at a concentration of 3 mM.

After appropriately diluting the test sample with assay buffer (20- and 125-fold dilution for assay with and without metabolism, respectively), 280 μL of the diluted sample was poured into the well of a 96-well microplate on ice. At least triplicate wells were used for each sample. Then, 10 μL of the AChE working solution was added to the diluted sample and the sample was preincubated at 37 °C for 30 min to allow AChE inhibitors present in the sample to exert their effect. After preincubation, 10 μL of the ACh working solution was added to the sample on ice and the sample was incubated at 37 °C for 60 min to allow Ch to be released from ACh by the enzymatic activity of non-inhibited AChE. After incubation, an aliquot (100 μL) of the sample was mixed with 100 μL of acetonitrile to terminate the enzymatic activity of AChE. The concentration of Ch in the final solution was measured by LC–MS. A control, prepared with assay buffer instead of the diluted sample, and a blank, prepared with assay buffer instead of both the diluted sample and the AChE working solution, were also tested using the same procedure. The anti-AChE activity of each sample was calculated using the following equation:

$$\text{Anti-AChE activity} = \frac{\text{Ch}_{\text{control}} - \text{Ch}_{\text{sample}}}{\text{Ch}_{\text{control}} - \text{Ch}_{\text{blank}}} \quad \text{(Eq. 1)}$$

where $\text{Ch}_{\text{control}}$, $\text{Ch}_{\text{sample}}$, and Ch_{blank} are the Ch concentrations in the control, sample, and blank, respectively.

2.5 Quantification of choline, diazinon, and diazinon-oxon, and identification of metabolites

Concentrations of Ch, diazinon, and diazinon-oxon were measured with a hybrid quadrupole-orbitrap mass spectrometer (Q Exactive, Thermo Fisher Scientific Inc., Waltham, MA, USA) coupled to an LC system (UltiMate 3000, Thermo Fisher Scientific). The detailed procedure is described in Text S1. Metabolites were identified under the same LC conditions as those used for quantification of diazinon and diazinon-oxon. Two measurement modes were used: scan mode (Full MS, resolution = 70,000, scan range = 50–500 *m*/*z*) and targeted MS/MS mode (Targeted-MS^2, resolution = 70,000, collision energy = 10–50 eV) under both positive and negative ion modes.

2.6 In silico *prediction of sites of metabolism*

To predict the molecular sites of metabolism targeted by cytochrome P450 (CYP), we used four freely available web-based *in silico* tools: FAME 2 on the GLORY platform (Universität Hamburg, https://nerdd.zbh.uni-hamburg.de/glory/),[31, 32] RS-WebPredictor (Rensselaer Polytechnic Institute, http://reccr.chem.rpi.edu/Software/RS-WebPredictor/),[33] SMARTCyp (University of Copenhagen, https://smartcyp.sund.ku.dk/mol_to_som),[34] and SOMP (Institute of Biomedical Chemistry, Russian Academy of Medical Sciences, http://www.way2drug.com/SOMP/). Each site of metabolism was ranked by using each of the tools, and the site with the smallest average rank was considered to be the most probable one. The ranks in RS-WebPredictor, SMARTCyp, and SOMP were the average

ranks of nine, three, and five CYP isozymes, respectively.

3. Results and Discussion

3.1 Effects of metabolism on the anti-AChE activities of standard solutions of diazinon and diazinon-oxon

First, we examined the anti-AChE activities of standard solutions of diazinon and diazinon-oxon with or without metabolism. Without metabolism, the diazinon solution showed almost no anti-AChE activity within the concentration range examined (0.01–10 μM; Fig. 1a). However, with metabolism, the diazinon solution showed marked anti-AChE activity (IC_{50} = 0.30 μM) that increased in a dose-dependent manner. These findings are consistent with previous studies that have suggested that metabolic activation is likely the reason why thiophosphoryl group (P=S)–containing organophosphorus insecticides such as diazinon show high anti-AChE activities in assays conducted *in vivo*,[35-37] which inherently account for the effects of metabolism, but show very low or no anti-AChE activities in cell-independent assays conducted *in vitro*.[15, 20, 28] The diazinon-oxon solution showed high anti-AChE activity irrespective of whether the solution underwent metabolism,[28, 38] although the activity was higher without metabolism (IC_{50} = 0.10 μM) than with metabolism (IC_{50} = 0.36 μM) (Fig. 1b). Taken together, these findings indicate that metabolism changed the anti-AChE activities of both diazinon and diazinon-oxon, but whereas it increased the activity of diazinon solution, it decreased the activity of diazinon-oxon solution. The clear implication here is that conventional *in vitro* cell-independent AChE activity assays alone, which do not take into account the effects of metabolism, are not suitable for fully evaluating the anti-AChE activity of orally ingested organophosphorus insecticides. Therefore, AChE activity assays that take into account the effects of metabolism are clearly needed.

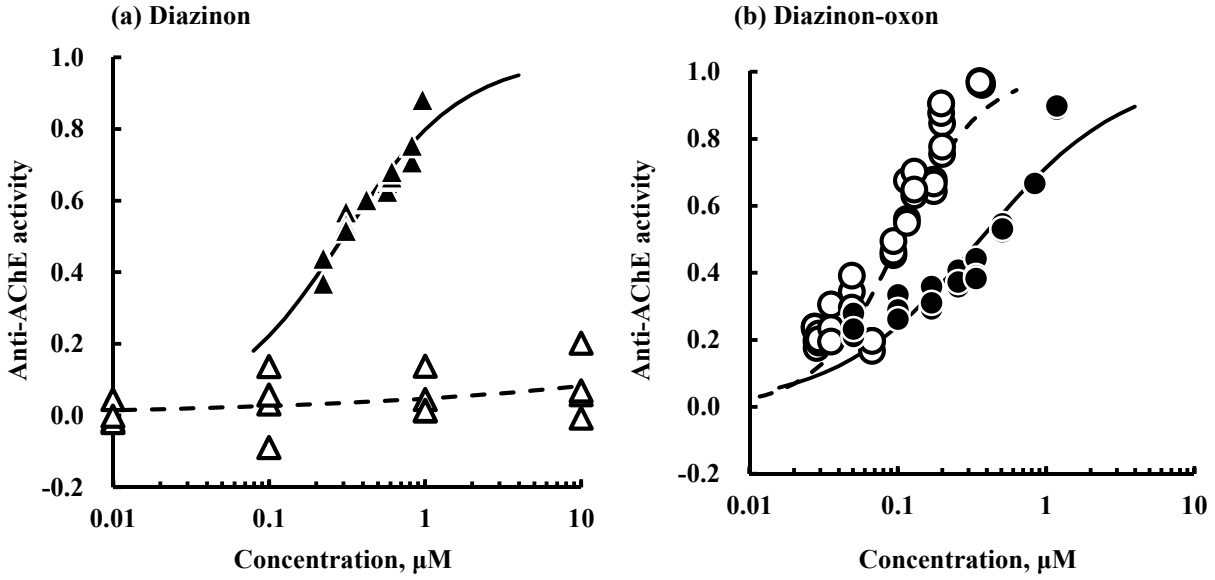

Fig. 1 Anti-acetylcholinesterase (AChE) activities of standard solutions of diazinon (a) and diazinon-oxon (b). Open and closed symbols represent direct (without metabolism) and indirect (with metabolism) anti-AChE activities, respectively. Direct anti-AChE activities of diazinon and diazinon-oxon are cited from our previous paper.[15] Note that the concentrations for indirect anti-AChE activity are those before metabolism.

Hereafter, the anti-AChE activity observed with metabolism is referred to as "indirect anti-AChE activity", whereas that observed without metabolism is referred to as "direct anti-AChE activity".

3.2 Effects of chlorination on the anti-AChE activity of a standard solution of diazinon

Next, we examined the effects of chlorination on the anti-AChE activity of diazinon solution over time. Within 10 min of the start of chlorination, all of the diazinon had been transformed by reaction with the free chlorine, resulting in the generation of diazinon-oxon (Fig. 2). The concentration of diazinon-oxon gradually decreased with chlorination time. The rapid decomposition of diazinon and its transformation to diazinon-oxon are in agreement with the published literature.[6, 7]

Although the diazinon solution did not show any direct anti-AChE activity before chlorination (Fig. 1a), it did after chlorination (Fig. 3a), indicating that diazinon was transformed to one or more products that had direct anti-AChE activity. Given that diazinon-oxon was produced by chlorination (Fig. 2) and that it showed direct anti-AChE activity (Fig. 1b), these findings strongly suggest that diazinon-oxon contributed to the observed anti-AChE activity of the diazinon solution after chlorination. In addition, because the highest conversion ratio from diazinon to diazinon-oxon was only 0.63, this indicates that some of the initially spiked diazinon was transformed to products other than diazinon-oxon. Accordingly, 2-isopropyl-6-methyl-pyrimidin-4-ol (IMP), diethyl phosphate, and dimethyl phosphate were detected in the diazinon solution after chlorination (Fig. S2). However, when we conducted the AChE activity assay using chemical standards of these three transformation products, we found that they showed no direct anti-AChE activity in the range of 0.1–10 μM (data not shown). Our finding regarding the anti-AChE activity of IMP is in agreement with a previous report by Čolović et al.[28] Therefore, we concluded that these three transformation products (IMP, diethyl phosphate, and dimethyl phosphate) did not contribute to the observed direct anti-AChE activity, indicating the presence of additional transformation products, one of which was suspected to be diazinon-oxon. Indeed, even though the concentration of dissolved organic carbon did not change during chlorination (data not shown), the total dissolved organic carbon derived from diazinon and the four identified transformation products after chlorination was always lower than the initial dissolved organic carbon (Fig. S2). Thus, the diazinon was transformed not only into the four identified products, but also into one or more additional products that may have direct anti-AChE activity.

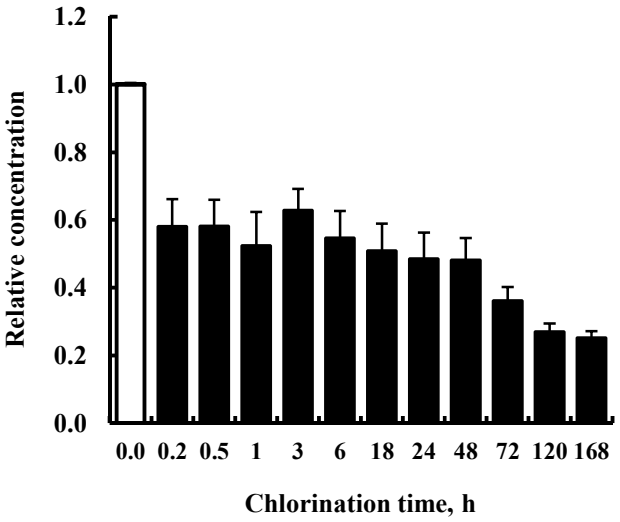

Fig. 2 Changes in the concentrations of diazinon (white column) and diazinon-oxon (black columns) relative to the initial diazinon concentration during chlorination. The initial concentration of diazinon was 38 μM. Error bars indicate standard deviations of 3 measurements.

We also found that the indirect anti-AChE activity of diazinon solution (Fig. 1b) was retained after chlorination (Fig. 3b). Because all of the diazinon was transformed immediately after the start of chlorination, the observed indirect anti-AChE activity indicates that some of the diazinon was transformed to products with indirect anti-AChE activity by reaction with free chlorine. Similar to the interpretation for direct anti-AChE activity, diazinon-oxon was suspected to contribute to the observed indirect anti-AChE activity because it was produced during chlorination (Fig. 2) and it was found to have indirect anti-AChE activity (Fig. 1b). The other three identified transformation products (i.e., IMP, diethyl phosphate, and dimethyl phosphate) showed no indirect anti-AChE activity in the range of 0.1–10 μM (data not shown). One or more unidentified transformation products with indirect anti-AChE activity may remain to be identified.

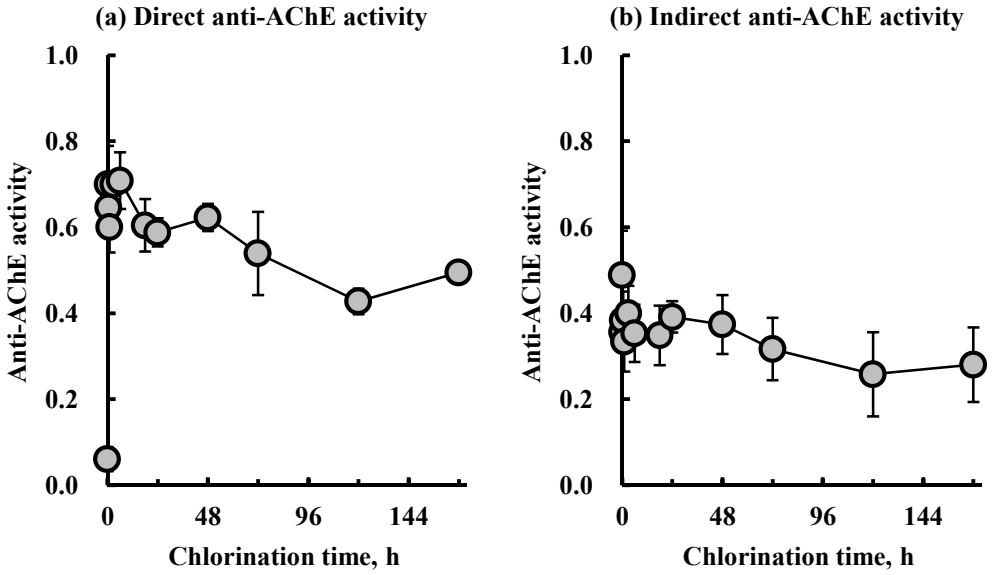

Fig. 3 Changes in the direct (a) and indirect (b) anti-acetylcholinesterase (AChE) activities of diazinon solution during chlorination. Error bars indicate standard deviations of 2 and 3 assays for direct and indirect anti-AChE activity, respectively.

3.3 Contribution of diazinon and diazinon-oxon to the direct and indirect anti-AChE activities observed after chlorination

To clarify whether the observed anti-AChE activities could be explained solely by the presence of diazinon and diazinon-oxon, we estimated the anti-AChE activity induced by diazinon and diazinon-oxon, without consideration of any transformation products. Because the dose–response curves for both the direct and indirect anti-AChE activities were not linear (Fig. 1), we concluded that the anti-AChE activity was not dose-additive; that is, the activity of a solution containing both diazinon and diazinon-oxon could not be calculated simply by summing the individual activities of diazinon and diazinon-oxon. Indeed, Čolović et al.[28] have reported that the direct anti-AChE activity of a solution containing both diazinon and diazinon-oxon was smaller than the sum of the individual activities at higher diazinon/diazinon-oxon concentrations. To estimate the total anti-AChE activity induced by a parent insecticide and its oxon coexisting in a sample, a mixture containing chemical standards of these compounds at the same concentrations as those in the sample should also be examined by anti-

AChE activity assay.[28, 39] However, in the present study, before chlorination the solution contained only diazinon and no diazinon-oxon, and after chlorination the solution contained only diazinon-oxon and no diazinon. Therefore, we determined the anti-AChE activity of diazinon from the data for the solution before chlorination, and we determined the activity of diazinon-oxon from the data for the solution after chlorination. For the solution before chlorination, we calculated the activity of diazinon from its concentration in the initial sample (Fig. 2) and the dose–response curve (Fig. 1a), being sure to take into account the dilution factor in the anti-AChE activity assay. For the solution after chlorination, we used the same procedure to calculate the activity of diazinon-oxon at every chlorination time.

Calculating the direct anti-AChE activity of the solution before chlorination revealed no direct anti-AChE activity, which was consistent with the observed activity (Fig. 4a). After chlorination, the direct anti-AChE activities calculated from the diazinon-oxon concentration were comparable with the observed direct anti-AChE activities. Together, these findings indicate that the observed direct anti-AChE activity is explained solely by the presence of diazinon-oxon, and that transformation products other than diazinon-oxon, which included both the identified and unidentified transformation products, did not contribute to the observed direct anti-AChE activity. When a similar analysis was conducted for indirect anti-AChE activity, the activities calculated from the concentration of diazinon in the solution before metabolism were comparable with the observed activities (Fig. 4b). After chlorination, the activities calculated from the concentration of diazinon-oxon in the solution before metabolism were comparable with the observed activities. Thus, both the direct and indirect anti-AChE activities could be explained solely by the presence of diazinon and diazinon-oxon before metabolism. This strongly suggests that diazinon-oxon, but not other transformation products, should be monitored in drinking water in addition to diazinon itself.

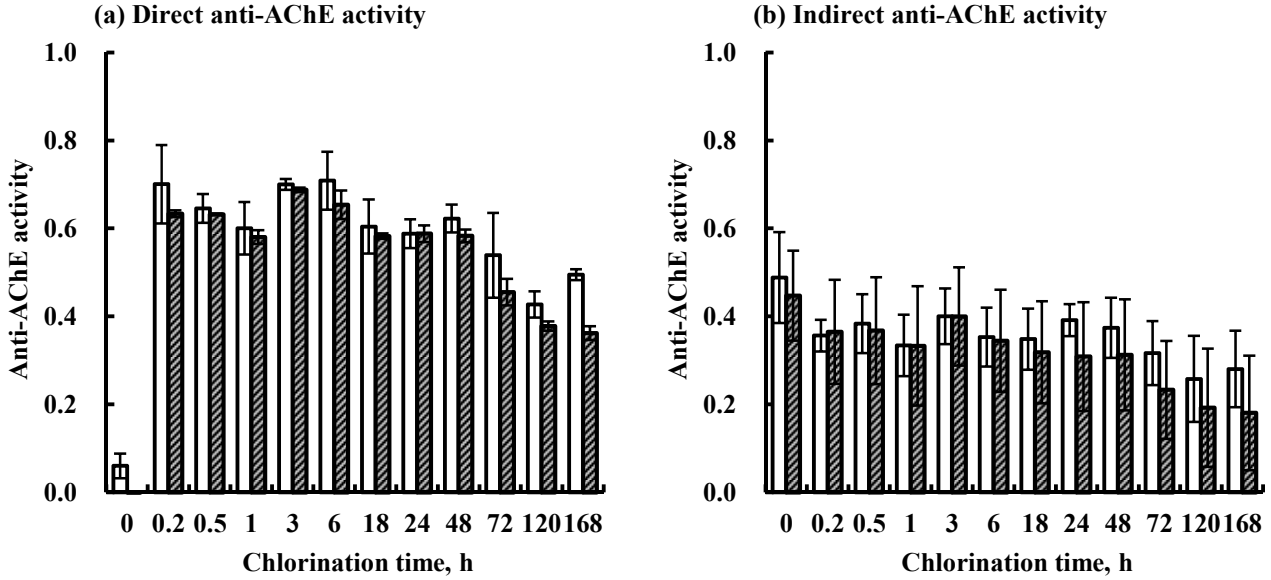

Fig. 4 Comparison of anti-acetylcholinesterase (AChE) activity during chlorination (open columns) with that calculated from the concentrations of diazinon or diazinon-oxon (hatched columns). Error bars indicate standard deviations of 2 and 3 assays for direct and indirect anti-AChE activities, respectively.

3.4 Identification of metabolites with anti-AChE activity generated by metabolism

Although neither diazinon nor diazinon-oxon was detected in the chlorinated solution after metabolism (Fig. S3), the solution still showed anti-AChE activity (Fig. 3b), indicating that diazinon and diazinon-oxon were metabolized to metabolites, some of which showed anti-AChE activity. Among the four identified transformation products observed before metabolism (diazinon-oxon, IMP, diethyl phosphate, and dimethyl phosphate), IMP alone was still detected after metabolism (Fig. S3). However, the dissolved organic carbon derived from IMP in the chlorinated solution after metabolism was approximately 1.5−2.0 mg/L, which was lower than the dissolved organic carbon of the initially spiked diazinon (5.4 mg/L). This means that a large part of the initially spiked diazinon and transformation products generated during chlorination was transformed to unidentified metabolites by metabolism. Because IMP, the only identified metabolite, had no anti-AChE activity, some of the unidentified metabolites must have been responsible for the observed anti-AChE activity.

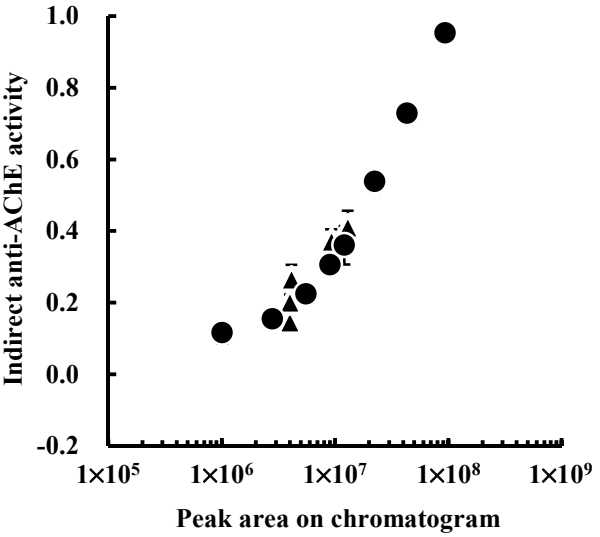

Fig. 5 Relationship between indirect anti-acetylcholinesterase (AChE) activity and area of Peak 2 on the liquid chromatography chromatogram detected after metabolism. Triangles and circles represent diazinon– and diazinon-oxon–derived Peak 2, respectively.

Just as in the chlorinated solutions, neither diazinon nor diazinon-oxon was detected after metabolism in the solutions used for determination of the dose–response curves of diazinon and diazinon-oxon (data not shown). Because the dose–response curves of diazinon and diazinon-oxon for indirect anti-AChE activity were comparable (Fig. S4), we hypothesized that during metabolism diazinon was first transformed to diazinon-oxon as an intermediate and then to one or more metabolites. Further examination revealed that both the diazinon and the diazinon-oxon solutions contained common metabolites, some of which had anti-AChE activity (Fig. S5). To identify these common metabolites, the solutions prepared for the dose–response curves were subjected to LC/MS analysis in scan mode. Two peaks not observed for the control solution were observed on the total ion chromatograms of the diazinon and diazinon-oxon solutions, which we

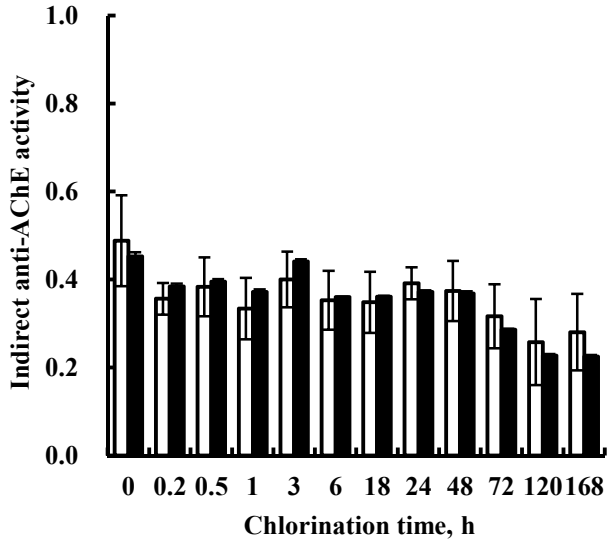

Fig. 6 Comparison of indirect anti-acetylcholinesterase (AChE) activity during chlorination (white columns) with that calculated from the area of Peak 2 on the liquid chromatography chromatogram (black columns). Error bars indicate standard deviations of 3 assays.

assumed were derived from metabolites with anti-AChE activity (Fig. S6). Comparisons of LC retention times and accurate *m/z* values with those of chemical standards revealed that the compound detected as Peak 1 was IMP; because IMP did not show anti-AChE activity, this peak was discounted. To evaluate whether or not the compound detected as Peak 2 had anti-AChE activity, we plotted the indirect anti-AChE activities of the dose–response curve solutions against the area of Peak 2 on the LC chromatograms detected in the solutions after metabolism, and we found that the area of Peak 2 was correlated with the indirect anti-AChE activities of the solutions (Fig. 5). Moreover, the plots for the diazinon and the diazinon-oxon solutions fell on the same curve. This observation strongly suggests that the metabolite corresponding to Peak 2 showed anti-AChE activity. Furthermore, for each chlorinated sample, the anti-AChE activity supposed to be induced by the metabolite was calculated by combining the dose–response curve (Fig. 5) and the area of Peak 2 on the LC chromatogram detected for each solution (Fig. S7), and then compared with the observed indirect anti-AChE activity. The calculated anti-AChE activity was almost the same as the observed one at every chlorination time (Fig. 6), strongly supporting the hypothesis that the metabolite detected as Peak 2 had anti-AChE activity.

To identify the metabolite, LC/MS analysis of Peak 2 was conducted. The three most probable candidate molecular formulae of the metabolite were estimated from the accurate *m*/*z* value and are shown in Table S2. Among these formulae, because $C_{12}H_{22}O_5N_2P$ alone satisfied the accuracy of the apparatus used in the present study (error in $m/z \leq 3$ ppm), the molecular formula of the metabolite was concluded to be $C_{12}H_{21}O_5N_2P$. Judging from the comparison of molecular formulae of diazinon-oxon ($C_{12}H_{21}O_4N_2P$) and the metabolite, the metabolite was most likely a compound that was generated by the addition of an oxygen atom to the diazinon-oxon molecule. Thus, chemical structures resulting from the mono-oxidation of diazinon-oxon were selected as candidates, under the assumption that the aromatic ring was not cleaved (Fig. S8).

To further identify the metabolite, we conducted an MS/MS analysis of Peak 2 with different collision energy values (0, 20, 30, 40, and 50 eV). To calculate the number of fragment ions corresponding to those in the tandem mass spectra of Peak 2 (isolate window = 0.4), a rule-based (Mass Frontier 7.0, HighChem, Bratislava, Slovakia) and a substructure-based (MAGMa, Netherlands eScience Centre, http://www.emetabolomics.org/magma) algorithm for MS/MS analysis were applied to each candidate structure. The MS/MS analysis by using a combination of the software with different annotation algorithms assigned the largest number of fragment ions (Fig. S9–S12) to four of the structures (Fig. S8a–d); thus, these structures were retained on the candidate list.

CYP is capable of catalyzing the oxidative biotransformation of most drugs,[40] and of facilitating a great variety of oxygen insertion processes into organic compounds.[41] Judging from the preparation method described in the datasheet provided by the manufacturer, the S9 mix used in the present study was a supernatant prepared by centrifugation of homogenized rat hepatic cells at $9000 \times g$; therefore, we assumed that it included CYP. This suggests that CYP likely contributed to the transformation of

diazinon-oxon to the metabolite detected as Peak 2. To narrow down the candidate structures, we used four web-based *in silico* tools to predict sites of CYP-mediated metabolism on the diazinon-oxon molecule (Table 1, see Text S2 for detailed discussion). The average ranks of Structures S8b and S8d were comparable and clearly smaller than those of Structures S8a and S8c. Accordingly, the metabolite that was detected as Peak 2 and that showed anti-AChE activity was likely either diethyl 6-(hydroxymethyl)-2-(propan-2-yl)pyrimidin-4-yl phosphate (Structure S8b) or diethyl 2-(2-hydroxypropan-2-yl)-6-methylpyrimidin-4-yl phosphate (Structure S8d). The former[42] and latter[42, 43] compound are both reported from *in vivo* and *in vitro* experiments to be metabolites of diazinon, and both compounds are reported to induce direct anti-AChE activity,[42] which supports our estimation.

Table 1 Comparison of ranks obtained using four web-based in silico prediction tools for the identified candidate structures of the metabolite with anti-acetylcholinesterase activity.

	S8a	S8b	S8c	S8d
	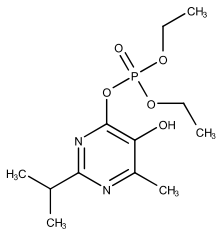	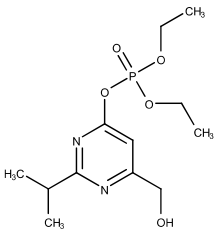	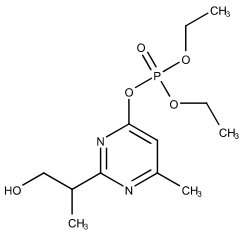	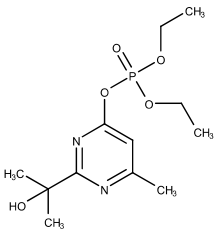
FAME 2	2	3	4	1
RS-WebPredictor	2	1	4	3
SMARTCyp	4	1	3	2
SOMP	3	2	4	1
Average rank	2.8	1.8	3.8	1.8

4. Conclusions

In the present study, to evaluate the toxicity of the organophosphorus insecticide diazinon after oral ingestion in humans, we incorporated metabolism into an *in vitro* cell-independent AChE activity assay. Using this assay, we found that the anti-AChE activities of diazinon and diazinon-oxon were dramatically changed via metabolism by enzymes contained in the S9 fraction; that is, this metabolism increased the anti-AChE activity of diazinon but reduced that of diazinon-oxon. This suggests that *in vitro* cell-independent assays to estimate toxicity after oral ingestion should ideally take into consideration the effects of metabolism.

Diazinon reacted rapidly with free chlorine and was completely transformed within 10 min of the start of chlorination. Some of the diazinon was transformed to diazinon-oxon. The diazinon-containing solution had no anti-AChE activity before chlorination, but had it after chlorination, and the activity was found to gradually decrease with chlorination time. With metabolism, diazinon solution before chlorination had anti-AChE activity, and this activity gradually decreased during chlorination. Anti-AChE activities calculated from the concentration of either diazinon or diazinon-oxon in the solution and from dose–response curves for chemical standards of the compounds were comparable with observed activities at every chlorination time regardless of whether the solution had

undergone metabolism. Thus, the observed anti-AChE activities were attributable solely to the presence of diazinon and diazinon-oxon in the solution before metabolism, suggesting that diazinon-oxon, but not other transformation products, should also be included in drinking water regulations.

Analysis using a combination of MS/MS and *in silico* site-of-metabolism prediction tools suggested that the compound that was generated through metabolism and was responsible for the observed indirect anti-AChE activity of the solution was a compound that was generated by mono-oxidation of a diazinon-oxon molecule; namely, either diethyl 6-(hydroxymethyl)-2-(propan-2-yl)pyrimidin-4-yl phosphate or diethyl 2-(2-hydroxypropan-2-yl)-6-methylpyrimidin-4-yl phosphate. However, because these compounds are produced via metabolism in the human body after oral ingestion of diazinon, their presence in drinking water need not be monitored and regulated.

Associated content

Supporting Information:

Fig. S1 Chemical structures. Table S1 Composition of stock solution of S9 mix. Text S1 Quantification methods. Fig. S2 Concentrations of DOC during chlorination. Fig. S3 Concentrations of DOC during chlorination after metabolism. Fig. S4 Indirect AChE activity induced by diazinon and diazinon-oxon. Fig. S5 Possible transformations of diazinon during chlorination and metabolism. Fig. S6 Comparison of LC chromatograms. Fig. S7 Changes in the area of Peak 2 on the LC chromatograms. Table S2 Candidate molecular formulae for Peak 2. Fig. S8 Candidate chemical structures of Peak 2. Figs. S9–12 Tandem mass spectrometry spectra of Peak 2 and assignment of fragment ions. Text S2 Results and interpretation of *in silico* site-of-metabolism analyses. Table S3–6 Results of FAME 2, RS-WebPredictor, SMARTCyp, and SOMP.

Acknowledgments

This research was supported in part by a Health and Labour Sciences Research Grant (19LA0501) from the Ministry of Health, Labour and Welfare of Japan, and by the Fuso Innovative Technology Fund.

References

(1) Kameya, T., Saito, M., Kondo, T., Toriumi, W., Fujie, K., Matsushita, T., and Takanashi, H. (2012) Detection of fenitrothion and its degradation product 3-methyl-4-nitrophenol in water environment. *Journal of Water and Environment Technology 10*, 427-436.

(2) Wang, D., Singhasemanon, N., and Goh, K. S. (2017) A review of diazinon use, contamination in surface waters, and regulatory actions in california across water years 1992-2014. *Environmental Monitoring and Assessment 189*, 1-7.

(3) Masiá, A., Campo, J., Navarro-Ortega, A., Barceló, D., and Picó, Y. (2015) Pesticide monitoring

in the basin of Llobregat River (Catalonia, Spain) and comparison with historical data. *Science of The Total Environment 503-504*, 58-68.

(4) Matsushita, T., Morimoto, A., Kuriyama, T., Matsumoto, E., Matsui, Y., Shirasaki, N., Kondo, T., Takanashi, H., and Kameya, T. (2018) Removals of pesticides and pesticide transformation products during drinking water treatment processes and their impact on mutagen formation potential after chlorination. *Water research 138*, 67-76.

(5) Kamel, A., Byrne, C., Vigo, C., Ferrario, J., Stafford, C., Verdin, G., Siegelman, F., Knizner, S., and Hetrick, J. (2009) Oxidation of selected organophosphate pesticides during chlorination of simulated drinking water. *Water research 43*, 522-534.

(6) Duirk, S. E., Desetto, L. M., and Davis, G. M. (2009) Transformation of Organophosphorus Pesticides in the Presence of Aqueous Chlorine: Kinetics, Pathways, and Structure−Activity Relationships. *Environmental Science & Technology 43*, 2335-2340.

(7) Li, W., Wu, R., Duan, J., Saint, C. P., and van Leeuwen, J. (2016) Impact of prechlorination on organophosphorus pesticides during drinking water treatment: Removal and transformation to toxic oxon byproducts. *Water research 105*, 1-10.

(8) Ohashi, N., Tsuchiya, Y., Sasano, H., and Hamada, A. (1994) Ozonation products of organophosphorous pesticides in water. *Japanese Journal of Toxicology and Environmental Health 40*, 185-192.

(9) Wu, J., Lan, C., and Chan, G. Y. S. (2009) Organophosphorus pesticide ozonation and formation of oxon intermediates. *Chemosphere 76*, 1308-1314.

(10) Zamy, C., Mazellier, P., and Legube, B. (2004) Phototransformation of selected organophosphorus pesticides in dilute aqueous solutions. *Water research 38*, 2305-2314.

(11) Ibanez, M., Sancho, J. V., Pozo, O. J., and Hernandez, F. (2006) Use of liquid chromatography quadrupole time-of-flight mass spectrometry in the elucidation of transformation products and metabolites of pesticides. Diazinon as a case study. *Analytical and bioanalytical chemistry 384*, 448-457.

(12) Kouloumbos, V. N., Tsipi, D. F., Hiskia, A. E., Nikolic, D., and van Breemen, R. B. (2003) Identification of photocatalytic degradation products of diazinon in TiO2 aqueous suspensions using GC/MS/MS and LC/MS with quadrupole time-of-flight mass spectrometry. *Journal of the American Society for Mass Spectrometry 14*, 803-817.

(13) Calza, P., Massolino, C., and Pelizzetti, E. (2008) Light induced transformations of selected organophosphorus pesticides on titanium dioxide: Pathways and by-products evaluation using LC–MS technique. *Journal of Photochemistry and Photobiology A: Chemistry 199*, 42-49.

(14) Magara, Y., Aizawa, T., Matsumoto, N., and Souna, F. (1994) Degradation of pesticides by chlorination during water purification. *Water Science & Technology 30*, 119-128.

(15) Matsushita, T., Fujita, Y., Omori, K., Huang, Y., Matsui, Y., and Shirasaki, N. (2020) Effect of chlorination on anti-acetylcholinesterase activity of organophosphorus insecticide solutions and contributions of the parent insecticides and their oxons to the activity. *Chemosphere 261*, 127743.

(16) Iwafune, T., Inao, K., Horio, T., Iwasaki, N., Yokoyama, A., and Nagai, T. (2010) Behavior of paddy pesticides and major metabolites in the Sakura River, Ibaraki, Japan. *Journal of Pesticide*

Science advpub, 1001130109-1001130109.

(17) Yin, L., Wang, B., Yuan, H., Deng, S., Huang, J., Wang, Y., and Yu, G. (2017) Pay special attention to the transformation products of PPCPs in environment. *Emerging Contaminants 3*, 69-75.

(18) Kiefer, K., Müller, A., Singer, H., and Hollender, J. (2019) New relevant pesticide transformation products in groundwater detected using target and suspect screening for agricultural and urban micropollutants with LC-HRMS. *Water research 165*, 114972.

(19) Zahn, D., Mucha, P., Zilles, V., Touffet, A., Gallard, H., Knepper, T. P., and Frömel, T. (2019) Identification of potentially mobile and persistent transformation products of REACH-registered chemicals and their occurrence in surface waters. *Water research 150*, 86-96.

(20) Tahara, M., Kubota, R., Tokunaga, H., Nakazawa, H., and Nishimura, T. (2008) The behaviour and cholinesterase inhibitory activity of fenthion and its products by light and chlorination. *Journal of Water Supply: Research and Technology-Aqua 57*, 143-151.

(21) Bavcon Kralj, M., Franko, M., and Trebše, P. (2007) Photodegradation of organophosphorus insecticides – Investigations of products and their toxicity using gas chromatography–mass spectrometry and AChE-thermal lens spectrometric bioassay. *Chemosphere 67*, 99-107.

(22) Čolović, M., Krstić, D., Petrović, S., Leskovac, A., Joksić, G., Savić, J., Franko, M., Trebše, P., and Vasić, V. (2010) Toxic effects of diazinon and its photodegradation products. *Toxicology Letters 193*, 9-18.

(23) Onodera, S., Hirose, Y., and Ishikura, S. (1995) Changes in Genetic and Enzymatic Inhibiting Effects of Organophosphorus Pesticides during Aqueous Chlorination. *Journal of Environmental Chemistry 5*, 65-71.

(24) Ellman, G. L., Courtney, K. D., Andres, V., and Featherstone, R. M. (1961) A new and rapid colorimetric determination of acetylcholinesterase activity. *Biochemical Pharmacology 7*, 88-95.

(25) Maeda, H., Matsuno, H., Ushida, M., Katayama, K., Saeki, K., and Itoh, N. (2005) 2,4-Dinitrobenzenesulfonyl Fluoresceins as Fluorescent Alternatives to Ellman's Reagent in Thiol-Quantification Enzyme Assays. *Angewandte Chemie International Edition 44*, 2922-2925.

(26) Sabelle, S., Renard, P.-Y., Pecorella, K., de Suzzoni-Dézard, S., Créminon, C., Grassi, J., and Mioskowski, C. (2002) Design and Synthesis of Chemiluminescent Probes for the Detection of Cholinesterase Activity. *Journal of the American Chemical Society 124*, 4874-4880.

(27) Liu, W., Yang, Y., Cheng, X., Gong, C., Li, S., He, D., Yang, L., Wang, Z., and Wang, C. (2014) Rapid and sensitive detection of the inhibitive activities of acetyl- and butyryl-cholinesterases inhibitors by UPLC–ESI-MS/MS. *Journal of Pharmaceutical and Biomedical Analysis 94*, 215-220.

(28) Čolović, M. B., Krstić, D. Z., Uščumlić, G. S., and Vasić, V. M. (2011) Single and simultaneous exposure of acetylcholinesterase to diazinon, chlorpyrifos and their photodegradation products. *Pesticide Biochemistry and Physiology 100*, 16-22.

(29) Maron, D. M., and Ames, B. N. (1983) Revised methods for the Salmonella mutagenicity test. *Mutation Research/Environmental Mutagenesis and Related Subjects 113*, 173-215.

(30) Asha, S., and Vidyavathi, M. (2010) Role of human liver microsomes in *In vitro* metabolism of

drugs—a review. *Applied Biochemistry and Biotechnology 160*, 1699-1722.

(31) de Bruyn Kops, C., Stork, C., Šícho, M., Kochev, N., Svozil, D., Jeliazkova, N., and Kirchmair, J. (2019) GLORY: Generator of the Structures of Likely Cytochrome P450 Metabolites Based on Predicted Sites of Metabolism. *Frontiers in Chemistry 7*.

(32) Stork, C., Embruch, G., Šícho, M., de Bruyn Kops, C., Chen, Y., Svozil, D., and Kirchmair, J. (2019) NERDD: a web portal providing access to in silico tools for drug discovery. *Bioinformatics 36*, 1291-1292.

(33) Zaretzki, J., Bergeron, C., Rydberg, P., Huang, T.-w., Bennett, K. P., and Breneman, C. M. (2011) RS-Predictor: A New Tool for Predicting Sites of Cytochrome P450-Mediated Metabolism Applied to CYP 3A4. *Journal of Chemical Information and Modeling 51*, 1667-1689.

(34) Rydberg, P., Rostkowski, M., Gloriam, D. E., and Olsen, L. (2013) The Contribution of Atom Accessibility to Site of Metabolism Models for Cytochromes P450. *Molecular Pharmaceutics 10*, 1216-1223.

(35) Oropesa, A. L., Pérez-López, M., and Soler, F. (2014) Characterization of plasma cholinesterase in rabbit and evaluation of the inhibitory potential of diazinon. *Ecotoxicology and Environmental Safety 100*, 39-43.

(36) Cong, N. V., Phuong, N. T., and Bayley, M. (2009) Effects of repeated exposure of diazinon on cholinesterase activity and growth in snakehead fish (Channa striata). *Ecotoxicology and Environmental Safety 72*, 699-703.

(37) Gokcimen, A., Gulle, K., Demirin, H., Bayram, D., Kocak, A., and Altuntas, I. (2007) Effects of diazinon at different doses on rat liver and pancreas tissues. *Pesticide Biochemistry and Physiology 87*, 103-108.

(38) Tahara, M., Kubota, R., Nakazawa, H., Tokunaga, H., and Nishimura, T. (2005) Use of cholinesterase activity as an indicator for the effects of combinations of organophosphorus pesticides in water from environmental sources. *Water research 39*, 5112-5118.

(39) Krstić, D. Z., Čolović, M., Bavcon kralj, M., Franko, M., Krinulović, K., Trebše, P., and VasiĆ, V. (2008) Inhibition of AChE by malathion and some structurally similar compounds. *Journal of Enzyme Inhibition and Medicinal Chemistry 23*, 562-573.

(40) Zanger, U. M., and Schwab, M. (2013) Cytochrome P450 enzymes in drug metabolism: Regulation of gene expression, enzyme activities, and impact of genetic variation. *Pharmacology & Therapeutics 138*, 103-141.

(41) Shaik, S., Kumar, D., de Visser, S. P., Altun, A., and Thiel, W. (2005) Theoretical Perspective on the Structure and Mechanism of Cytochrome P450 Enzymes. *Chemical Reviews 105*, 2279-2328.

(42) Machin, A. F., Rogers, H., Cross, A. J., Quick, M. P., Howell, L. C., and Janes, N. F. (1975) Metabolic aspects of the toxicology of diazinon. I. Hepatic metabolism in the sheep, cow, pig, guinea-pig, rat, turkey, chicken and duck. *Pesticide Science 6*, 461-473.

(43) Shishido, T., and Fukami, J.-i. (1972) Enzymatic hydrolysis of diazoxon by rat tissue homogenates. *Pesticide Biochemistry and Physiology 2*, 39-50.

Supporting information for:

A metabolism-coupled cell-independent acetylcholinesterase activity assay for evaluation of the effects of chlorination on diazinon toxicity

Taku Matsushita[†*], Yuji Kikkawa[‡], Kei Omori[‡],
Yoshihiko Matsui[†], and Nobutaka Shirasaki[†]

[†]Faculty of Engineering, Hokkaido University, N13W8, Sapporo 060-8628, Japan

[‡]Graduate School of Engineering, Hokkaido University, N13W8, Sapporo 060-8628, Japan

[*]Corresponding author: taku-m@eng.hokudai.ac.jp; +81–11–706–7279

Contents

- ✓ Fig. S1 Chemical structures of diazinon and diazinon-oxon. S3
- ✓ Table S1 Composition of stock solution of S9 mix. S3
- ✓ Text S1 Quantification of choline, diazinon, and diazinon-oxon. S4
- ✓ Fig. S2 Concentrations of DOC derived from diazinon during chlorination and the structures of three of its transformation products. S5
- ✓ Fig. S3 Concentrations of DOC derived from diazinon during chlorination after metabolism. S5
- ✓ Fig. S4 Indirect AChE activity induced by diazinon and diazinon-oxon. S6
- ✓ Fig. S5 Schematic diagram of possible transformations of diazinon during chlorination and metabolism. S6
- ✓ Fig. S6 Comparison of LC chromatograms of diazinon, diazinon-oxon, and control subjected to acetylcholinesterase activity assay after metabolism. S7
- ✓ Fig. S7 Changes in the area of Peak 2 on the LC chromatograms during chlorination after metabolism. S8
- ✓ Table S2 Candidate molecular formulae for the compound represented by Peak 2. S8
- ✓ Fig. S8 Candidate chemical structures of the metabolite detected as Peak 2. S9
- ✓ Fig. S9 Tandem mass spectrometry spectra of Peak 2 with different values of collision energy and assignment of fragment ions for Structure S8a. S10
- ✓ Fig. S10 Tandem mass spectrometry spectra of Peak 2 with different values of collision energy and assignment of fragment ions for Structure S8b. S11
- ✓ Fig. S11 Tandem mass spectrometry spectra of Peak 2 with different values of collision energy and assignment of fragment ions for Structure S8c. S12
- ✓ Fig. S12 Tandem mass spectrometry spectra of Peak 2 with different values of collision energy and assignment of fragment ions for Structure S8d. S13
- ✓ Text S2 Results and interpretation of in silico site-of-metabolism analyses. S14

- ✓ Table S3 Comparison of probabilities obtained using FAME 2 for the identified candidate structures of the metabolite with anti-AChE activity. S14
- ✓ Table S4 Comparison of ranks obtained using RS-WebPredictor for the identified candidate structures of the metabolite with anti-AChE activity. S14
- ✓ Table S5 Comparison of scores obtained using SMARTCyp for the identified candidate structures of the metabolite with anti-AChE activity. S15
- ✓ Table S6 Comparison of delta P values obtained using SOMP for the identified candidate structures of the metabolite with anti-AChE activity. S15

(a) Diazinon **(b) Diazinon-oxon**

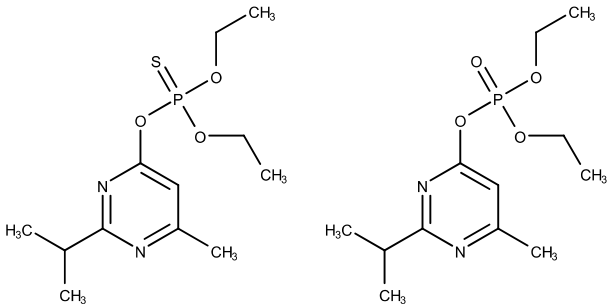

Fig. S1 Chemical structures of (a) diazinon and (b) diazinon-oxon.

Table S1 Composition of stock solution of S9 mix.

Component	Amount
S9	2 mL
glucose-6-phosphate	37.6 mg
β-NADPH	70.8 mg
β-NADH	53.2 mg
0.4 M $MgCl_2$ solution	400 μL
1.65 M KCl solution	400 μL
0.2 M phosphate buffer *	10 mL
Milli-Q water	8 mL

* Phosphate buffer	Amount
$NaH_2PO_4 \cdot 2H_2O$	15.7 g
$Na_2HPO_4 \cdot 12H_2O$	35.9 g
Milli-Q water	500 mL

Text S1 Quantification of choline, diazinon, and diazinon-oxon

The concentration of choline was measured by using a hybrid quadrupole-orbitrap mass spectrometer (MS; Q-Exactive, Thermo Fisher Scientific Inc., Waltham, MA, USA) coupled with a liquid chromatograph (LC; UltiMate 3000, Thermo Fisher Scientific). A 5-μL sample of the test solution was assayed with the LC equipped with a 100 mm × 2.1 mm Cortecs UPLC HILIC column (1.6-μm particle size, Waters Corporation, Milford, MA, USA). The mobile phase was a binary gradient of 100 mM ammonium formate in Milli-Q water (solvent A) and 100% acetonitrile (solvent B) at a flow rate of 200 μL/min as follows: begin with 95:5 (v/v) A/B, increase linearly to 60% B over a period of 0.75 min, hold at that ratio for 0.25 min, decrease linearly to 30% B over a period of 0.25 min, hold at that ratio for 1.25 min, and then decrease linearly to 5% B over a period of 3.5 min. The MS was operated in electrospray ionization mode (positive) with a spray voltage of 3.2 kV. The temperature of the capillary and electrospray ionization probe heater was 220 and 450 °C, respectively. The flow rate of the sheath gas, auxiliary gas, and sweep gas was 50, 15, and 0 units, respectively. The S-lens radio frequency level was set to 57. The concentration of choline was quantified in selected-ion-monitoring mode with m/z 104.1070 (resolution = 70,000). The detection limit for choline was 5 nM.

The concentrations of diazinon and diazinon-oxon were measured with the same apparatus as used for choline. A 5-μL sample of test solution was assayed with the LC equipped with a 50 mm × 2.1 mm Hypersil Gold column (1.9-μm particle size, Thermo Fisher Scientific). The mobile phase was a binary gradient of 2 mM ammonium formate in Milli-Q water (solvent A) and 100% methanol (solvent B) at a flow rate of 200 μL/min as follows: 99:1 (v/v) A/B for 2 min, increase linearly to 60% B over a period of 2 min, increase linearly to 75% B over a period of 5 min, increase linearly to 99% B over a period of 5 min, decrease linearly to 1% B over a period of 0.1 min, and then hold at that ratio for 1.9 min. The MS was operated in electrospray ionization mode (positive) with a spray voltage of 3.2 kV. The temperature of the capillary and electrospray ionization probe heater was 220 and 450 °C, respectively. The flow rate of the sheath gas, auxiliary gas, and sweep gas was 50, 15, and 0 units, respectively. The S-lens radio frequency level was set to 57. The concentrations of diazinon and diazinon-oxon were quantified in selected-ion-monitoring mode with m/z 305.1083 and 289.1312, respectively (resolution = 70,000). The detection limit was 3 nM both for diazinon and diazinon-oxon.

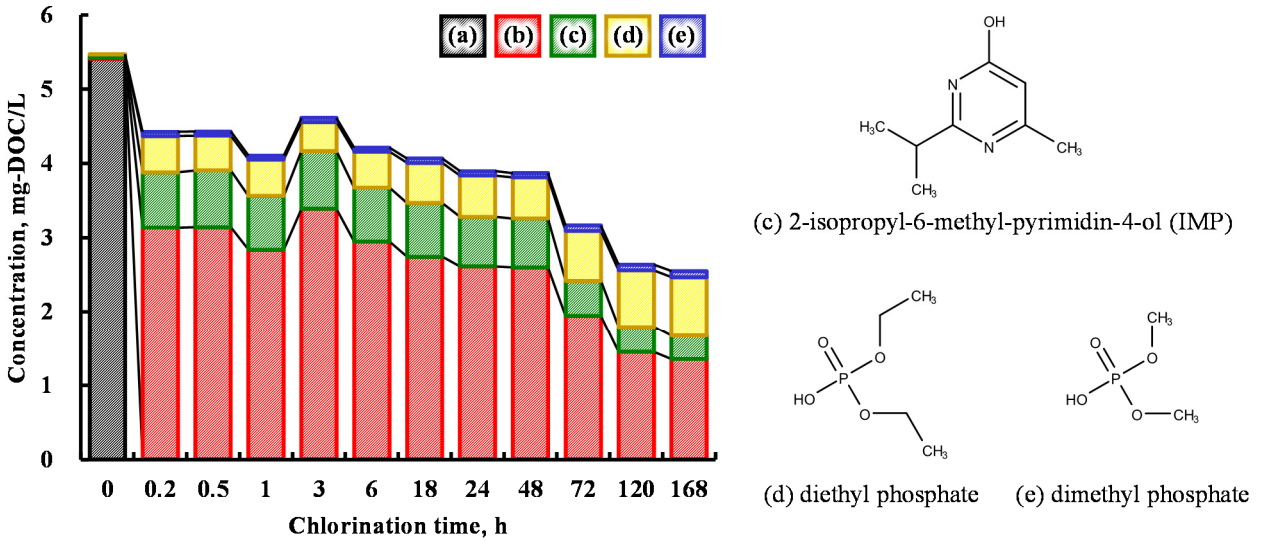

Fig. S2 Concentrations of dissolved organic carbon (DOC) derived from diazinon during chlorination and the structures of three of its transformation products. (a) Diazinon, (b) diazinon-oxon, (c) 2-isopropyl-6-methyl-pyrimidin-4-ol (IMP), (d) diethyl phosphate, and (e) dimethyl phosphate.

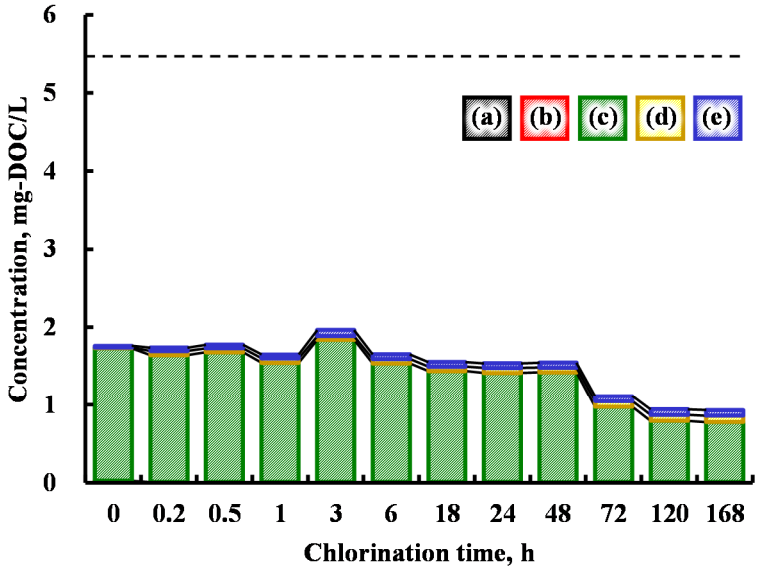

Fig. S3 Concentrations of dissolved organic carbon (DOC) derived from diazinon during chlorination after metabolism. (a) Diazinon, (b) diazinon-oxon, (c) 2-isopropyl-6-methyl-pyrimidin-4-ol (IMP), (d) diethyl phosphate, and (e) dimethyl phosphate. Dashed line indicates the DOC concentration of the initial sample (before chlorination) before metabolism.

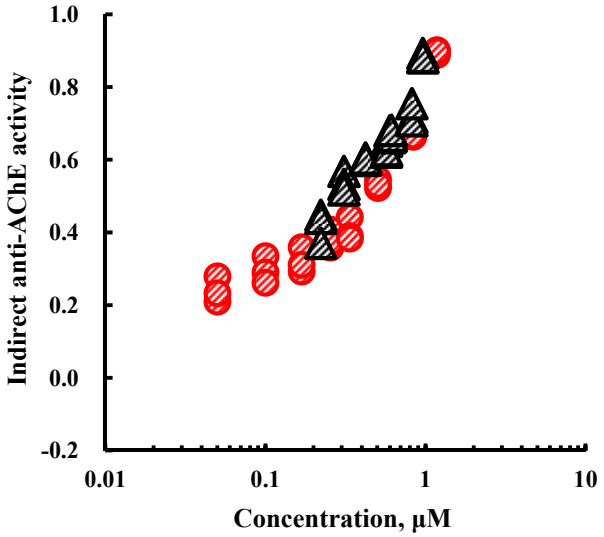

Fig. S4 Indirect anti-acetylcholinesterase (AChE) activity induced by diazinon (black triangles) and diazinon-oxon (red circles). The values are the same as those in Fig. 1. Note that the concentrations are before metabolism.

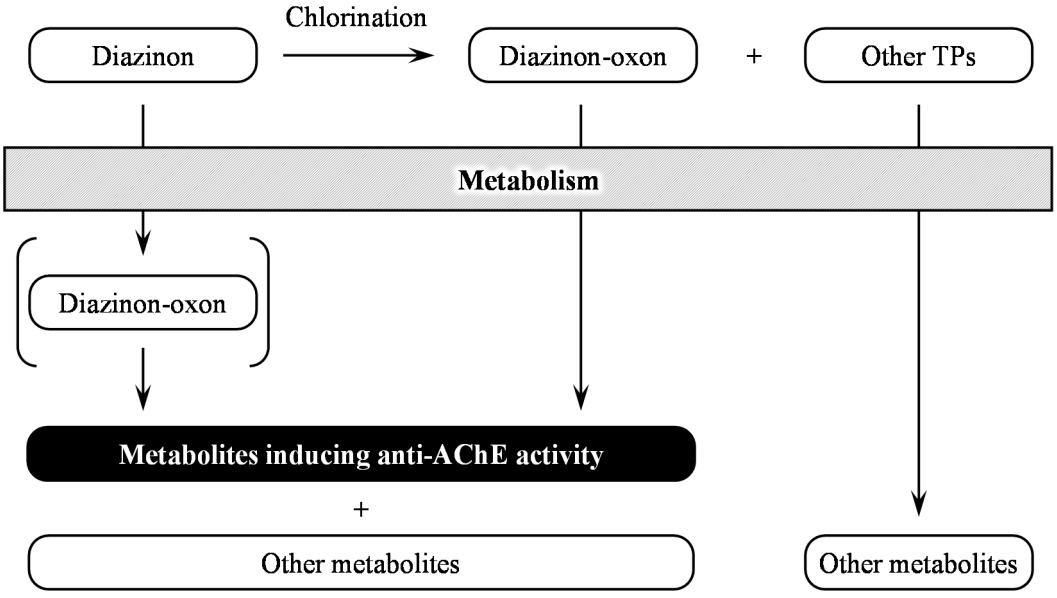

Fig. S5 Schematic diagram of possible transformations of diazinon during chlorination and metabolism. AChE, acetylcholinesterase; TPs, transformation products.

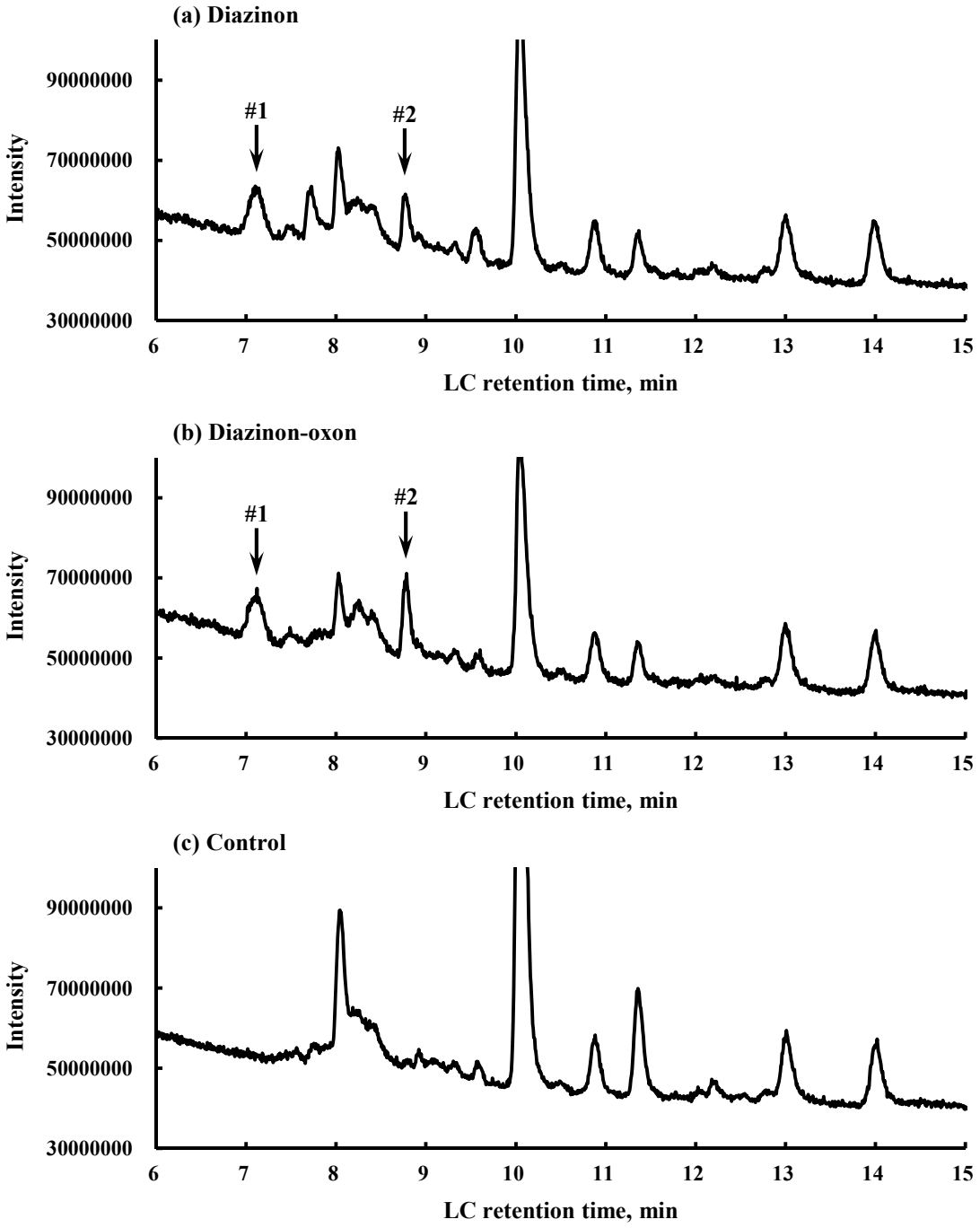

Fig. S6 Comparison of liquid chromatography (LC) chromatograms (positive ion mode) of (a) diazinon, (b) diazinon-oxon, and (c) control subjected to acetylcholinesterase activity assay after metabolism. The control sample was prepared as follows: 800 μL phosphate buffer was mixed with 2000 μL of the stock solution of S9 mix, and then incubated at 37 °C for 20 min in a shaking water bath. After that, 900 μL of the solution was immediately centrifuged for 60 min by using an ultracentrifuge.

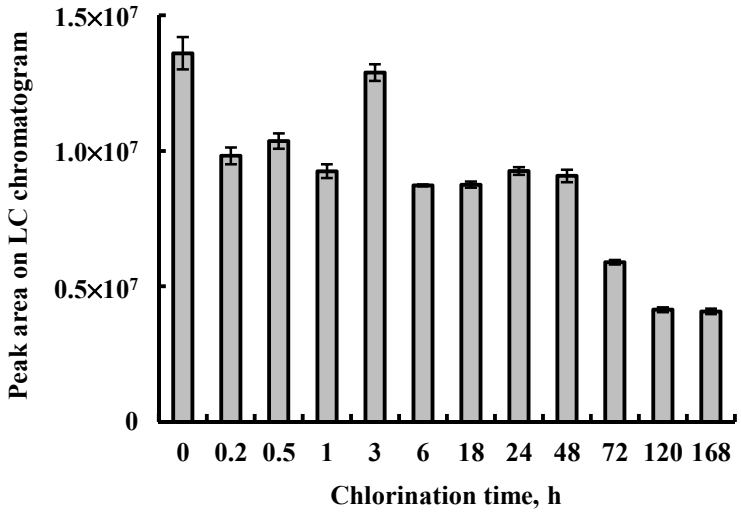

Fig. S7 Changes in the area of Peak 2 on the liquid chromatography chromatograms (positive ion mode) during chlorination after metabolism. Error bars indicate standard deviations of 3 measurements.

Table S2 Candidate molecular formulae for the compound represented by Peak 2 (m/z = 305.1256).

Molecular formula	Theoretical m/z	Error, ppm
$C_{12}H_{22}O_5N_2P$	305.1261	−1.6
$C_9H_{24}O_8NP$	305.1234	7.2
$C_{13}H_{21}O_8$	305.1231	8.2

Calculation condition: C≤14, H≤50, O≤10, N≤2, P≤1, and S≤1.

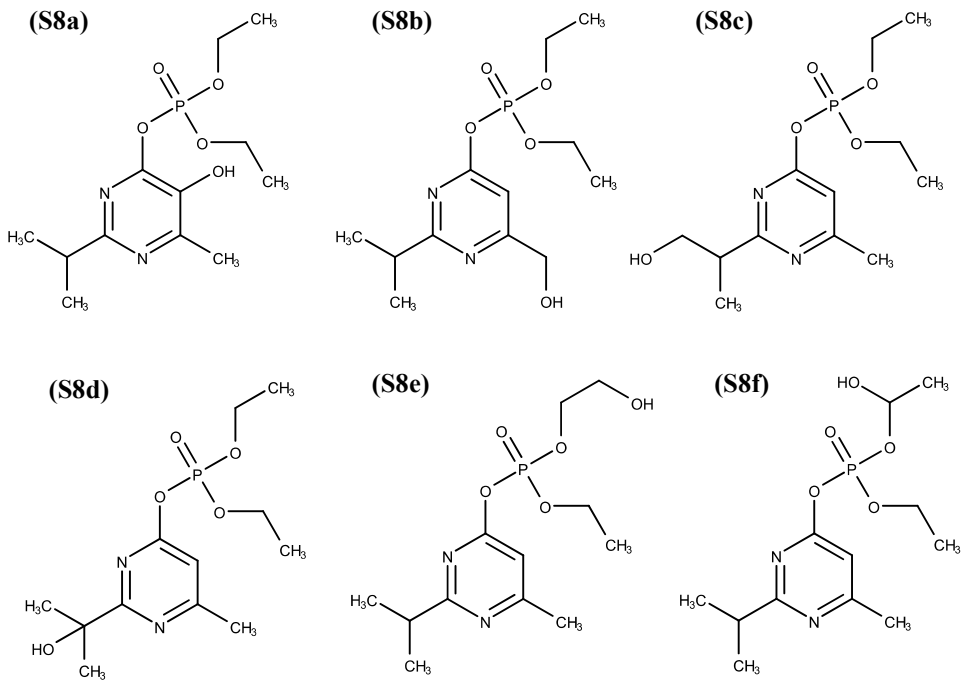

Fig. S8 Candidate chemical structures of the metabolite detected as Peak 2.

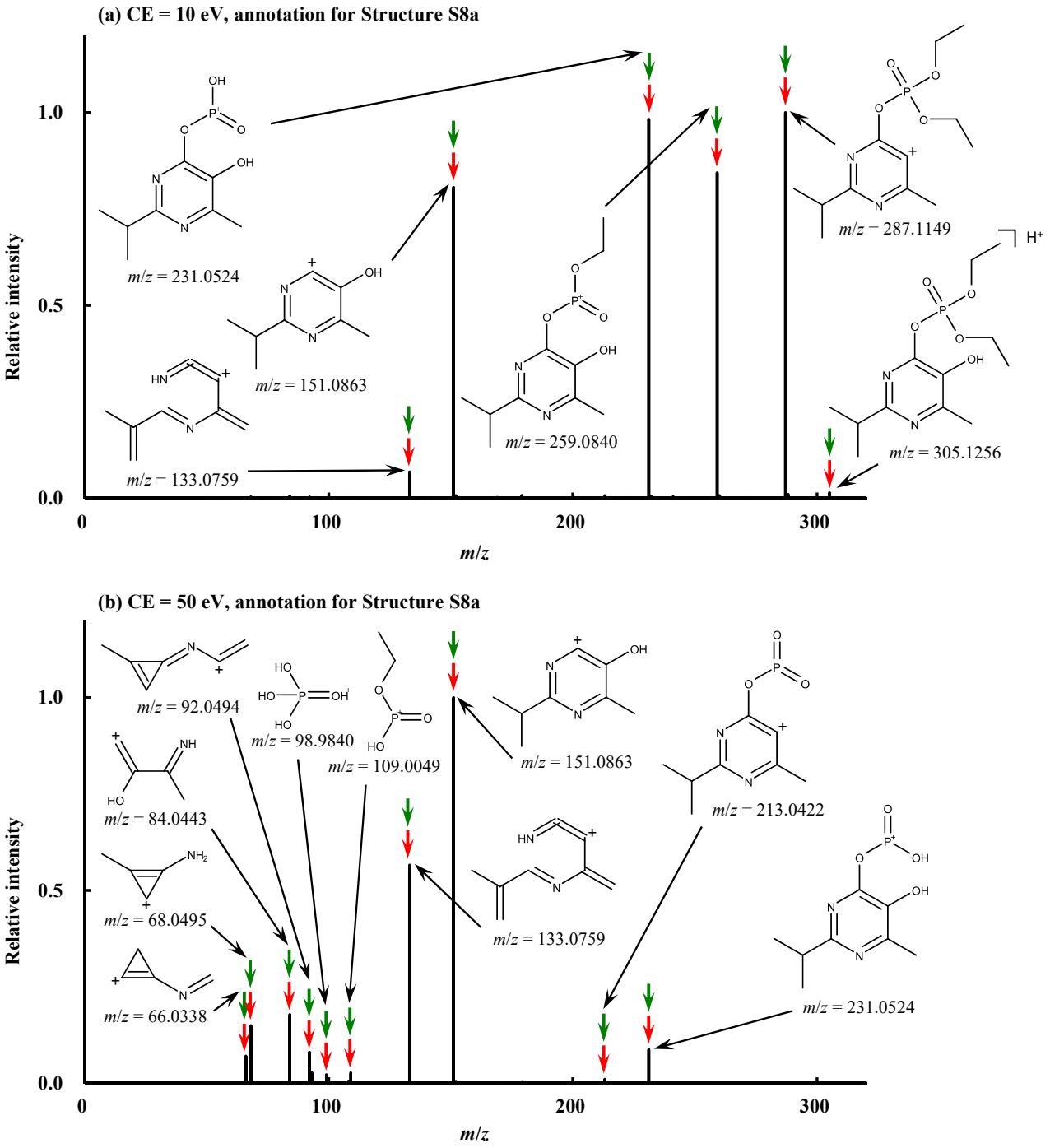

Fig. S9 Tandem mass spectrometry spectra of Peak 2 (m/z = 305.1256, positive ion mode) with different values of collision energy (CE) and assignment of fragment ions for Structure S8a. Red and green arrows represent fragment ions assigned with Mass Frontier and MAGMa, respectively.

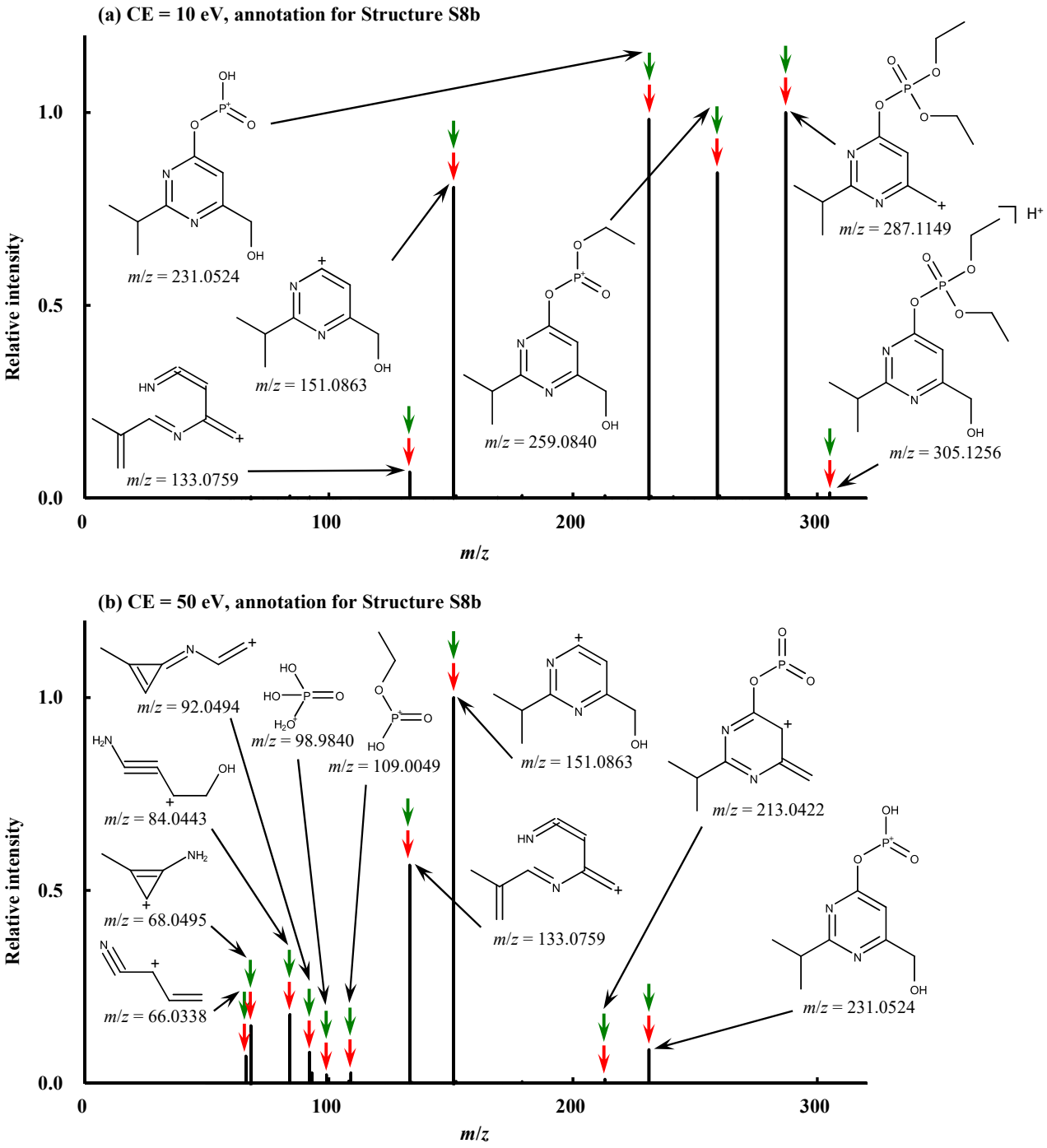

Fig. S10 Tandem mass spectrometry spectra of Peak 2 (m/z = 305.1256, positive ion mode) with different values of collision energy (CE) and assignment of fragment ions for Structure S8b. Red and green arrows represent fragment ions assigned with Mass Frontier and MAGMa, respectively.

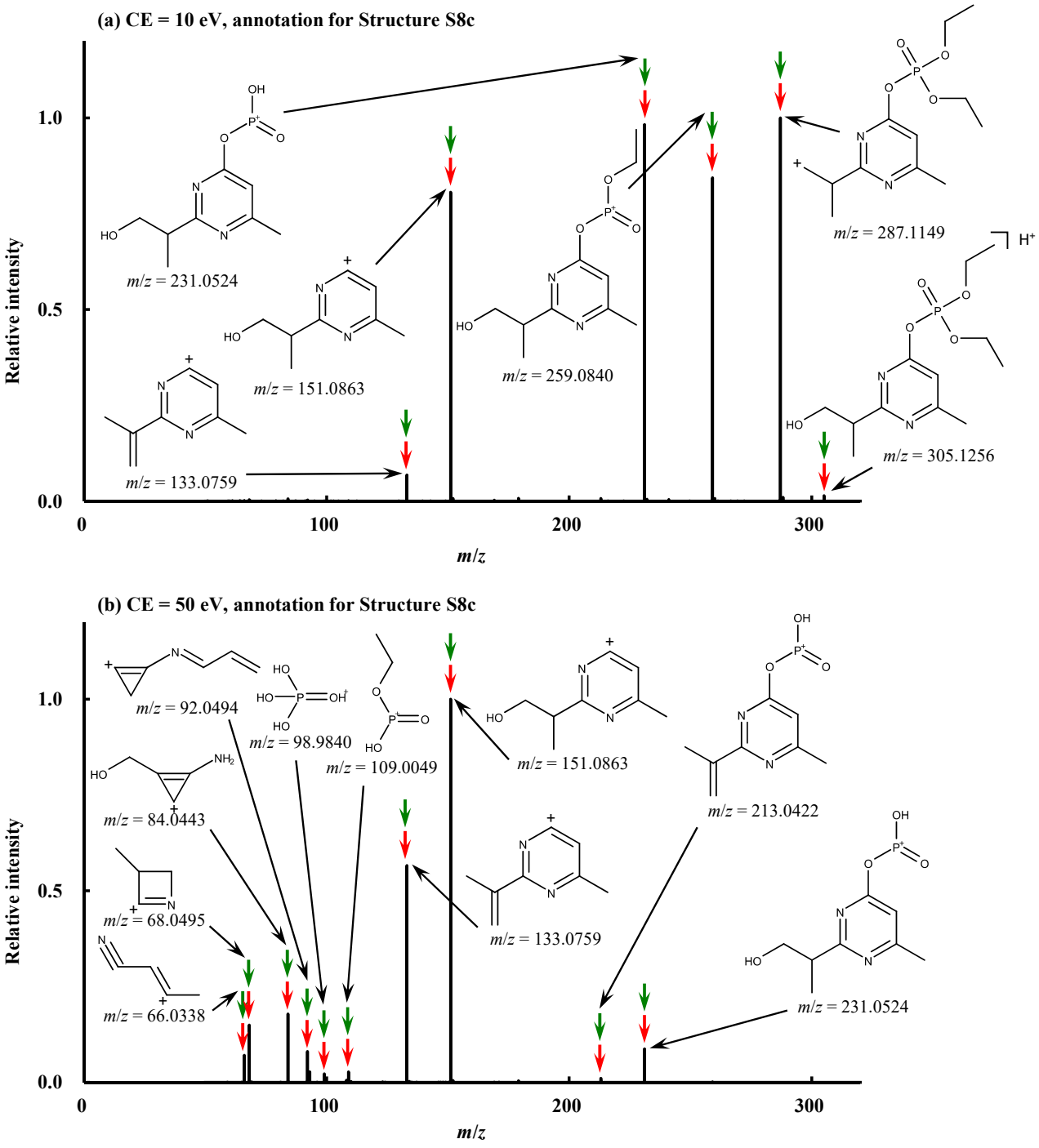

Fig. S11 Tandem mass spectrometry spectra of Peak 2 (m/z = 305.1256, positive ion mode) with different values of collision energy (CE) and assignment of fragment ions for Structure S8c. Red and green arrows represent fragment ions assigned with Mass Frontier and MAGMa, respectively.

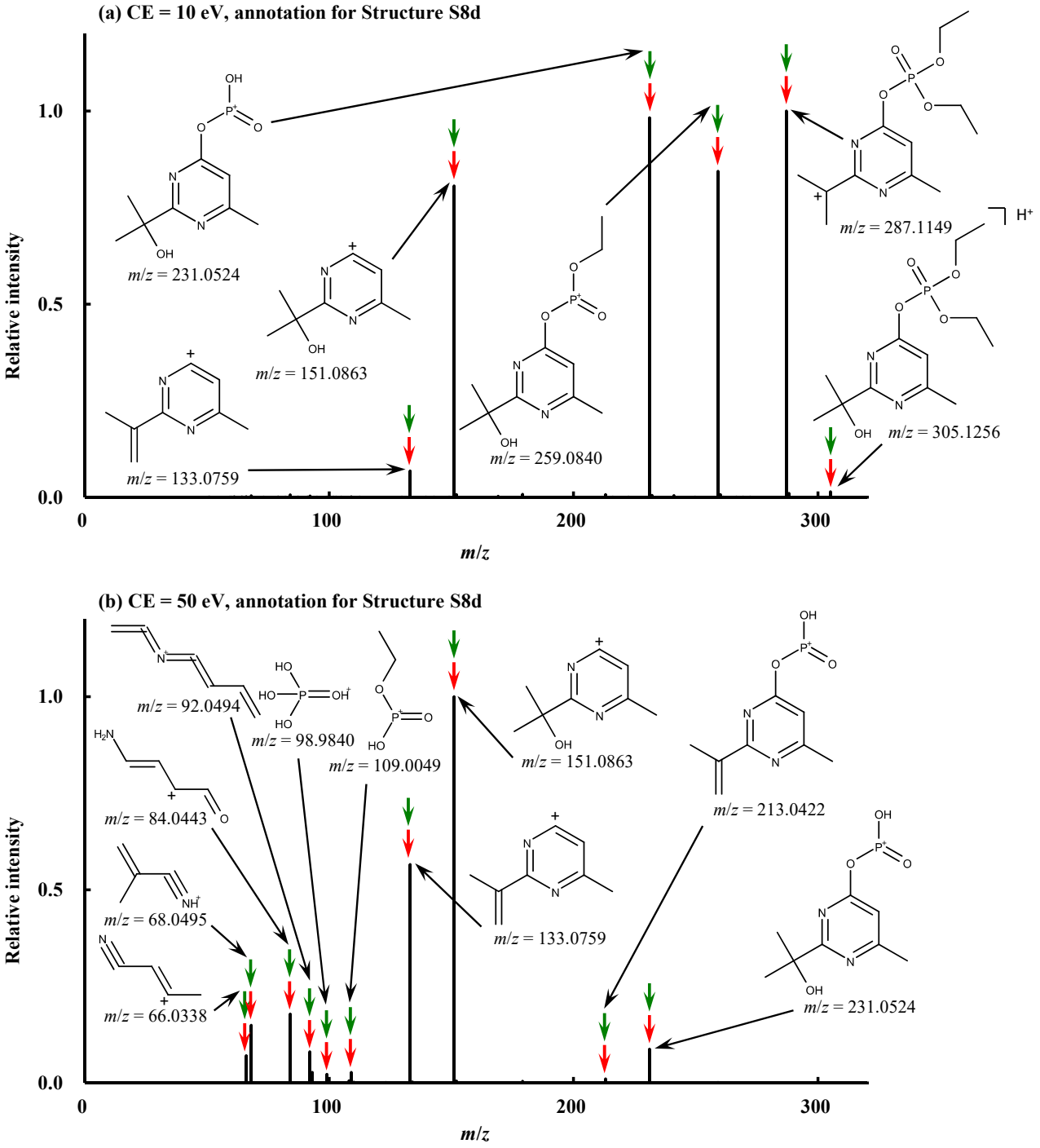

Fig. S12 Tandem mass spectrometry spectra of Peak 2 (m/z = 305.1256, positive ion mode) with different values of collision energy (CE) and assignment of fragment ions for Structure S8d. Red and green arrows represent fragment ions assigned with Mass Frontier and MAGMa, respectively.

Text S2 Results and interpretation of in silico *site-of-metabolism analyses*

FAst MEtabolizer 2 (FAME 2)[1] outputs for the four identified metabolite candidate structures (Table S3). Probabilities were generated for each atom in the structure by using the extra trees model (i.e., the percentage of trees that predicted the atom as a site of metabolism [SOM]); the higher the probability is, the more likely the structure is enzymatically produced by CYP. Structures S8a and S8d showed the largest probabilities, followed by S8b and S8c in that order.

Table S3 Comparison of probabilities obtained using FAME 2 for the identified candidate structures of the metabolite with anti-acetylcholinesterase activity. The higher the probability is, the smaller the rank is.

	S8a	S8b	S8c	S8d
	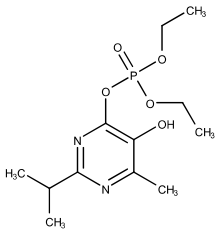	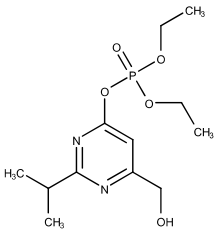	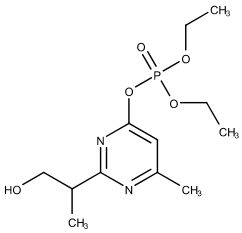	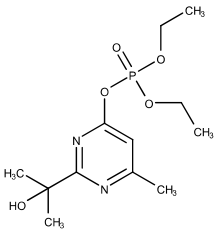
Probability	0.14	0.12	0.08	0.15
Rank	2	3	4	1

RS-WebPredictor[2] outputs for the top three predicted SOMs for each CYP isozyme for each candidate structure (Table S4). Structures not in the top 3 were assigned rank 4. S8a and S8b were ranked within the top 3 for almost all isozymes, whereas S8c and S8d were ranked below the top 3 for almost all isozymes. The candidate structures were ordered based on their average ranks.

Table S4 Comparison of ranks obtained using RS-WebPredictor for the identified candidate structures of the metabolite with anti-acetylcholinesterase activity.

	S8a	S8b	S8c	S8d
	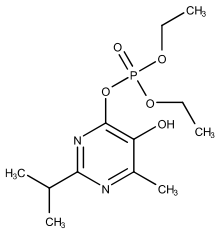	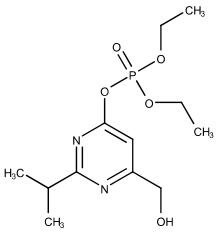	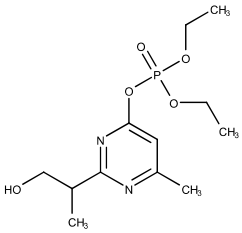	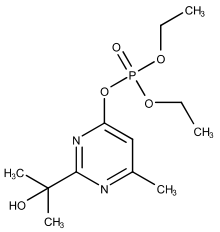
CYP1A2	3	2	4	4
CYP2A6	3	1	4	4
CYP2B6	2	1	4	4
CYP2C8	2	1	4	4
CYP2C9	2	1	4	4
CYP2C19	3	1	4	4
CYP2D6	4	1	4	4
CYP2E1	4	1	4	2
CYP3A4	3	1	4	4
Average	2.9	1.1	4.0	3.8
Average rank	2	1	4	3

SMARTCyp[3] outputs for the candidate structures (Table S5). A score was calculated by using the reactivity descriptor (an estimate of the energy required for the CYP under consideration to react with a given atom in the molecule) and the accessibility descriptor (the longest bond-path distance from the atom under consideration divided by the longest bond-path distance across the whole molecule). The atoms in the molecule were ranked by score, with the lowest score resulting in the lowest rank, and thus the highest probability of being a SOM. The scores for S8b and S8d were comparable for all CYP isozymes, and were always lower than those for S8a and S8c.

Table S5 Comparison of scores obtained using SMARTCyp for the identified candidate structures of the metabolite with anti-acetylcholinesterase activity. The lower the score is, the smaller the rank is.

		S8a	S8b	S8c	S8d
		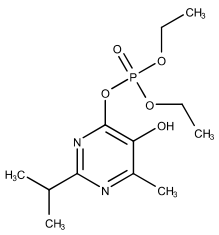	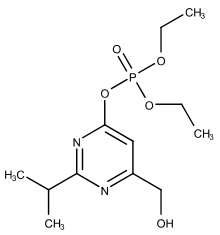	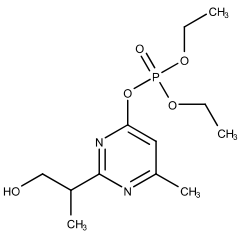	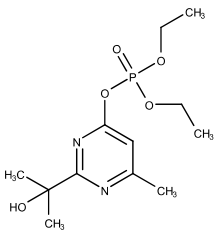
Score	CYP2C9	94	70	87	72
	CYP2D6	96	71	87	73
	CYP3A4	71	57	79	59
	Average	87	66	85	68
Average rank		4	1	3	2

SOMP[4] outputs for the candidate structures (Table S6). Delta P values were calculated by subtracting the probability that a given atom is not a SOM for the CYP isozyme under consideration from the probability that the atom is a SOM. Accordingly, the higher the delta P value is, the more likely the structure is enzymatically produced by the CYP. The delta P values of S8b and S8d were positive for all CYP isozymes, whereas those of S8a and S8c were negative for more than half of the CYP isozymes and were always smaller than those of S8b and S8d.

Table S6 Comparison of delta P values obtained using SOMP for the identified candidate structures of the metabolite with anti-acetylcholinesterase activity. The higher the delta P value is, the smaller the rank is.

		S8a	S8b	S8c	S8d
		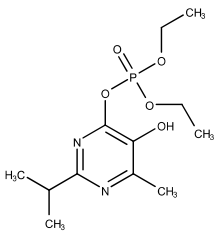	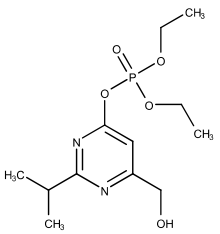	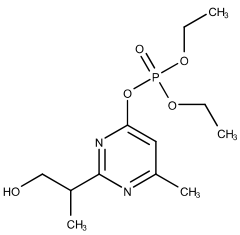	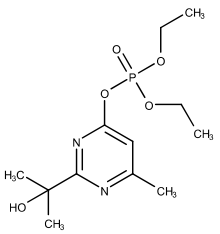
Delta P	CYP1A2	0.37	0.57	-0.20	0.88
	CYP2C19	-0.25	0.58	0.33	0.27
	CYP2C9	-0.29	0.65	-0.07	0.91
	CYP2D6	-0.17	0.17	-0.53	0.92
	CYP3A4	0.41	0.53	0.04	0.89
	Average	0.01	0.50	-0.09	0.77
Average rank		3	2	4	1

References

(1) Šícho, M., de Bruyn Kops, C., Stork, C., Svozil, D. and Kirchmair, J. (2017) FAME 2: simple and effective machine learning model of cytochrome P450 regioselectivity, *Journal of Chemical Information and Modeling*, **57**, 1832−1846.

(2) Zaretzki, J., Bergeron, C., Huang, T., Rydberg, P., Swamidass, S. J. and Breneman, C. M. (2013) RS-WebPredictor: a server for predicting CYP-mediated sites of metabolism on drug-like molecules, *Bioinformatics*, **29**, 497−498.

(3) Rydberg, P., Gloriam, G. E., Zaretzki, J., Breneman, C. and Olsen, L. (2010) SMARTCyp: a 2D method for prediction of cytochrome P450-mediated drug metabolism, *ACS Medicinal Chemistry Letters*, **1**, 96−100.

(4) http://www.way2drug.com/SOMP/interpr.php, visited on 29 June 2021.